AquaCode: Turning Transaction Platforms into Non-Invasive Liquid Quality Checker

Sijie Ji*†✉, Sheng Lyu*‡, Wenjian Li†, Wei Gao†
†California Institute of Technology ‡ Indenpendent Researcher
Email: {sijieji, wjli, weigao}@caltech.edu, lyusheng.nj@gmail.com

ABSTRACT

Existing liquid sensing solutions typically fail to achieve real-world scalability. Current channel-based methods (*e.g.*, RF, acoustics) approach this problem through a consumer-centric classification paradigm. However, their measurements become tightly coupled to non-repeatable channel responses and heterogeneous hardware. As a result, systems require massive, ad-hoc data collection to cover these variations, yet still fail to generalize across the practically infinite diversity of products. In this paper, we propose a paradigm shift to targeted verification and repurpose the identity tag as a sensing interface. We present *AquaCode*, the first liquid quality assessment system seamlessly integrated into retail checkout platforms. Instead of inferring liquid types via unstable channels, *AquaCode* harnesses Liquid-Solid Interface (LSI), a novel sensing modality that measures charge transfer dynamics directly at the outer container wall, making it immune to external multipath interference. Crucially, *AquaCode* leverages the checkout platform to provide standardized mechanical excitation, converting the erratic motion artifacts of handheld sensing into a deterministic signal source. This enables a robust verification model: the system compares the runtime LSI signal against a manufacturer-defined golden standard encoded in a low-cost passive tag. We design a specialized analog frontend to extract these faint, high-impedance signals and a lightweight algorithm for 1-to-1 verification. We achieve a recall of 0.905 for identifying low-quality drinks. We believe *AquaCode* offers a scalable path to ubiquitous liquid safety.

CCS CONCEPTS

• **Human-centered computing** → **Ubiquitous and mobile computing**; • **Hardware** → **Emerging interfaces**.

KEYWORDS

Liquid Quality Assessment, Liquid-Solid Interface, Non-Invasive Sensing Retail Authentication

ACM Reference Format:
Sijie Ji*†✉, Sheng Lyu*‡, Wenjian Li†, Wei Gao† . 2026. *AquaCode*: Turning Transaction Platforms into Non-Invasive Liquid Quality Checker. In *The 24th Annual International Conference on Mobile Systems, Applications and Services (MobiSys '26), June 21–25, 2026, Cambridge, United Kingdom.* ACM, New York, NY, USA, 14 pages. https://doi.org/10.1145/3745756.3809225

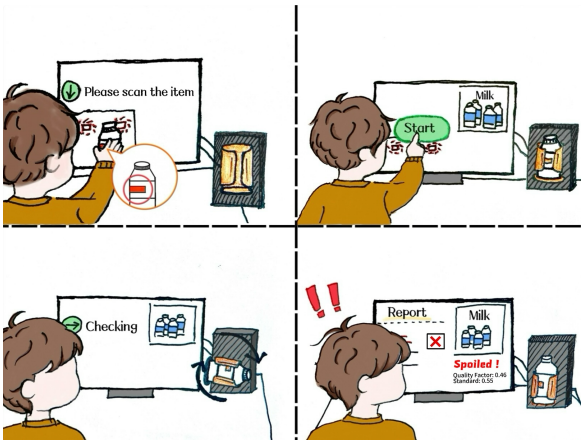

Figure 1: Scenarios of *AquaCode*. *AquaCode* performs 1-to-1 verification at the checkout platform. The platform retrieves the standard quality metric from the tag. The tag also serves as the interactive sensor to measure the real-time liquid physical state and *AquaCode* compares them against the reference metric.

1 INTRODUCTION

The quality and safety of liquids pose significant health and economic risks to the public. Conventional checks, including expiration dates and visual inspection, often fail to detect spoilage or contamination that occurs during storage and transit [1, 14, 18, 26, 32]. *These failures reveal that the current verification mechanisms are fundamentally misplaced in space and time.* Factory-side quality control is too early while relying on consumers to detect anomalies post-purchase is too late and shifts the burden of safety onto the victim. This disconnect motivates the need for in-situ verification that accompanies a product through the supply chain.

We argue that the optimal intervention point of liquid quality check is the transaction platform, which naturally serves as the bridge between manufacturers and consumers. The checkout platforms have been standard infrastructure in any retail context [2, 8]. Moreover, they offer a unified and controlled environment for liquid verification, thereby eliminating the variability introduced by portable devices.

Recent solutions in liquid sensing have exploited various signals, including Wi-Fi, RFID, acoustics, and optical signals [13, 21, 29]. These channel-based methods model the propagation channel in the presence of the liquid. However, they fail to provide a repeatable metric given different placements, container shape and ambient

*Sijie Ji and Sheng Lyu are co–first authors and contributed equally to this work.

MobiSys '26, June 21–25, 2026, Cambridge, United Kingdom

ACM ISBN 979-8-4007-2027-7/26/06.
https://doi.org/10.1145/3745756.3809225

environment. And this leads to a fundamental *scalability problem*. The root cause of such barrier is that the liquid serves as part of the propagation fields and contributes to only a minor fraction of the overall channel response. In other words, the SNR of the liquid-induced perturbations is inherently low, making models tightly coupled to the specific devices and scenes they were trained on.

We then naturally ask: *how can liquid quality verification be embedded into checkout platforms in a way that is effective, non-invasive, and scalable across the entire supply chain?* Our key observation stems from the identity tag [1], one of the most successful and scalable technologies in retail environments. It works not because of better scanners, but because the signal is manufacturer-defined, explicitly encoded, and read by fixed infrastructure, which guarantees a stable label across diverse environments. However, the current tag is fundamentally retrospective. It retrieves historical data regarding what the product was when it left the factory, yet remains blind to what the product is at the moment of purchase, which changes with temperature, storage conditions, contamination, dilution, or adulteration. Effective liquid check thus requires not only recovering a manufacturer-defined identifier, but *comparing the liquid's real-time physical state against a trusted reference*, without opening the container and without relying on unstable environmental channels.

This gap motivates us to reimagine what a product tag can be. First, we leverage the tag's storage capacity to embed the manufacturer's supervision. Since manufacturers possess the ground-truth data of their pristine products, they can encode this "golden standard" directly into the tag's digital payload. Second, we transform the physical form of the tag to be "measurable". It evolves from a simple label into a novel sensing interface that responds to in-situ liquid state.

Motivated by this, we propose *AquaCode*, the first-of-its-kind liquid quality sensing system that can be seamlessly integrated into the transaction platforms. At a high level, *AquaCode* transforms the identity tag into a dynamic, measurable physical signature that functions as a robust, environment-invariant code. As shown in Fig. 1, when the consumer places the product on the checkout platform, the tag captures the liquid's real-time electrochemical state under the controlled conditions, enabling precise 1-to-1 verification. However, translating this concept into a robust system requires addressing three fundamental challenges:

First, *what is the optimal physical modality for liquid verification at the checkout?* The failure of the existing channel methods [13, 21, 25, 29, 30, 41] motivates a fundamentally different physical sensing mechanism that bypasses the channel. Inspired by the recent advances in electrochemistry [16, 23, 36, 42], we exploit a new approach that harnesses the physical charge transfer dynamics at the liquid–solid interface (LSI) to uncover the underlying properties of the liquid. It requires no independent power supply that can be seamlessly attached to products. Remarkably, this phenomenon is highly sensitive to variations in liquid composition and, critically, exhibits intrinsic resilience to electromagnetic and RF disturbances. With controlled contact mechanics, the system achieves robust performance under typical retail conditions.

[1] An identity tag is a label affixed to a product container that serves as a unique physical identifier for manufacturer-defined specifications.

Second, *how can we reliably acquire meaningful LSI signals given their distinct electrical characteristics?* A naive approach employing off-the-shelf operational amplifiers fails due to the formation of the Electric Double Layer (EDL) at the interface. The EDL creates an extremely high internal impedance (GΩ to TΩ), causing severe impedance mismatch with conventional electronics. Furthermore, the slow signal drift and low-frequency noise, arising from electrochemical reactions, will be mixed with the DC drift and offsets on vanilla amplifiers, making it difficult to distinguish genuine interface changes from instrument error. Consequently, we must design a specialized analog front-end capable of extracting these faint, high-impedance signals with significant noise. We use electrometer-grade op-amps with ultra-low bias current and ultra-high input impedance. Through a transimpedance amplifier with feedback elements, we reliably convert tiny currents into stable, measurable ones.

Finally, *how can we translate AquaCode into an effective, scalable, and easy-to-deploy end-to-end solution? AquaCode* is designed as a scalable system that integrates seamlessly with existing transaction platforms. We tackle this challenge through two complementary paths. First, we adopt a low-cost tag design that imposes no additional burden on manufacturers or customers. The labelling materials are ubiquitous in retail settings and cost less than $0.01 per bottle. Second, *AquaCode* incorporates a lightweight liquid assessment model. This model extracts physically meaningful features from LSI, achieving sub-millisecond latency. The features are then mapped to quantitative quality metrics. This lightweight design enables real time deployment on edge devices, supporting scalable and practical liquid quality assessment.

Extensive evaluations validate *AquaCode*'s effectiveness. We offer unique quantitative quality metrics for each liquid and map them into three categories: high-quality, low-quality and counterfeit. For off-the-shelf beverages (*e.g.* tea, juice, soda, milk, energy drinks), it achieves recall rates of 97.5%, 90.5%, and 85.8% for the three categories, respectively. For specialized liquids (*e.g.* oils, pharmaceuticals, perfumes), it achieves F1 scores of 98.8% (high-quality) and 89.7% (low-quality). The system remains stable over different measurements, with a 0.95 correlation under environmental (temperature, humidity) and operational variations (rotation speed), and maintains 90.5% accuracy across glass and plastic containers. With 5 ms latency and less than 500 KB memory, *AquaCode* enables real-time, scalable deployment in retail checkout systems. Overall, our results confirm that *AquaCode* delivers reliable, efficient, and scalable liquid authentication at the transaction platforms.

Contribution: We summarize the contributions:

❶ We present the first liquid quality assessment system seamlessly integrated into checkout platforms.

❷We repurpose product tags for liquid quality assessment. *AquaCode* extends the current identity tag to the first physical-state tag, with a manufacturer-defined electrochemical signature that can be verified at scale.

❸ We characterize charge-transfer dynamics at the LSI as a reliable, high-SNR signature of liquid state, identify its invariance properties, and design dedicated sensing hardware that captures these signatures.

❹ We build and evaluate an end-to-end system, demonstrating the effectiveness and efficiency of *AquaCode* through extensive real-world experiments.

2 PROBLEM SCOPE

From Classification to Verification: Existing liquid sensing research [4, 7, 17, 25, 30, 46] has predominantly framed the problem as a *classification* task. In this section, we analyze the limitations of this traditional formulation and articulate why a shift to a verification-based paradigm, anchored by the transaction platform, is essential for real-world scalability.

The prevailing paradigm in mobile liquid sensing is **user-centric classification**. The learning goal is to map the mobile sensor readings to the label from a predefined set of categories. We argue that this formulation is fundamentally flawed for counterfeit detection and quality assurance due to two reasons: ❶ The space of commercial liquids is effectively unbounded and constantly evolving. Existing works typically rely on ad-hoc data collection, either small-scale datasets collected in controlled labs or crowdsourced data from end-users. Both are fundamentally unscalable. The model will invariably fail when encountering a new device or a slightly different store environment that was not represented in the training set. ❷ Classification models are designed to learn boundaries *between* distinct classes (*e.g.*, separating Coke from Water). They maximize inter-class variance. However, counterfeit detection requires identifying *intra-class* anomalies. A slightly diluted spirit or a spoiled juice is statistically very close to the genuine product. A standard classifier, optimizing for broad accuracy, will likely group the "slightly bad" liquid into the "good" class, failing the core safety objective.

To address these pitfalls, *AquaCode* **reframes the problem space from generic classification to targeted verification**. Instead of asking "What is this liquid?", we ask: "Is this liquid consistent with the digital claim of its tag?" We model the problem as a *1-to-1 matching* task. Let $\mathcal{M}_{\text{m}}$ be the signal measured at the checkout, and $\mathcal{M}_{\text{r}}$ be the golden standard signature retrieved from the tag for that specific Stock Keep Unit (SKU) measured by the manufacturers. And then we verify the liquid by, *i.e.*, $\mathcal{R} = \mathcal{D}(\mathcal{M}_{\text{m}}, \mathcal{M}_{\text{r}}) < \epsilon$, where ϵ is the threshold. The threshold is unique for every SKU and defined by the manufacturer. Notably, manufacturers would determine them based on product properties (*e.g.*, liquid type and expiration dates), assigning stricter margins to high-value products and more tolerant thresholds to everyday goods. Clearly, the system does not need to know or learn what the liquid is. It only compares the current measurement against the reference carried by the bottle itself. A new product can be introduced simply by encoding its reference into its tag, requiring no model retraining. Furthermore, by narrowing the scope to a single SKU, we can set tight, product-specific tolerance thresholds, allowing the system to detect minute changes in concentration or quality that would be ignored by a broad classifier. Importantly, the variations of the containers, including the shape, materials, thickness, *etc*, are effectively neutralized, as the referenceinherently accounts for the specific SKU. The verification logic prioritizes the relative deviation from the established reference standard instead of relying on absolute physical values. This ensures *AquaCode* remains robust

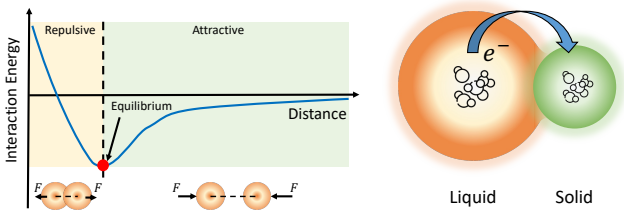

Figure 2: Electrons transfer between two media.

across diverse products and accommodates minor manufacturing tolerances within the same SKU.

Limitations of the Current Art: Vision-based methods[13, 33] analyze optical features but are strictly limited by lighting conditions and container transparency. Wireless sensing leverages RF signals (Wi-Fi, RFID, mmWave) [25, 29, 30, 37, 38, 41] or acoustic signals [21, 34] to interact with liquids. While innovative, these channel-based approaches face two fundamental limitations in practice. ❶ **Environmental Dependency:** RF and acoustic channels are susceptible to multipath effects and ambient noise. For instance, RF-EATS [11] and LiquID [7] require precise antenna placement or specific container geometries, causing performance degradation in dynamic environments. ❷ **Hardware Heterogeneity:** The reliance on user devices (smartphones) introduces inconsistent signal responses due to varying hardware specifications [22, 31], necessitating complex calibration or large-scale data collection for deep learning models [21]. In summary, while these methods might detect broad changes, their sensitivity to the environment makes them incapable of defining a stable "Golden Standard" across different contexts.

Why LSI?: Unlike the existing techniques vulnerable to environmental interference, LSI measures charge transfer dynamics strictly at the molecular liquid-solid interface. This makes the signal *intrinsic* to the liquid and immune to external noise. Moreover, while LSI generation requires relative motion, the transaction platform turns this dependency into an asset. Our operational model assumes a standardized mechanical excitation: the checkout motor drives the bottle with a uniform, deterministic rotation speed. By replacing stochastic human handling with precise motor control, we ensure that any signal variation is strictly due to liquid properties, not motion irregularity. This effectively decouples the sensing process: with environmental noise excluded by LSI physics and motion artifacts eliminated by the platform, any deviation in the signal can be rigorously attributed to the liquid's quality, enabling precise 1-to-1 verification.

3 LIQUID-SOLID INTERFACE (LSI)

3.1 Principles

Charge Transfer: The charge transfer is driven by contact electrification and ion displacement at the interface during mechanical excitation. Contact Electrification (CE) occurs when a liquid, such as water or an organic solvent, contacts a solid material like glass or polymer. When the liquid comes into contact with the solid container, atoms from both materials approach each other [39]. As the inter-atomic distance r decreases, the electron clouds overlap, as shown in Fig. 2. According to the electron cloud potential well

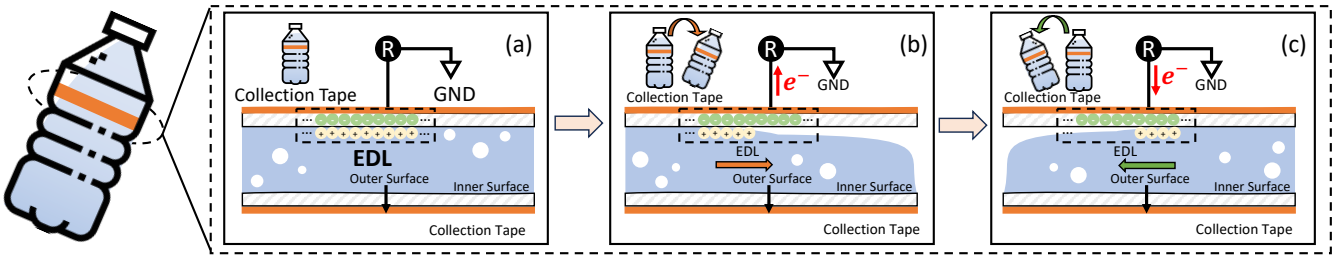

Figure 3: The Process of LSI Charge Transfer.

model [39], electrons overcome the energy barrier and transfer between the phases to equalize chemical potentials. The probability of this transfer, $T(r)$, is governed by the specific electronic structure of the molecules:

$$T(r) = \frac{1}{1 + \exp\left(\beta(r - r_c)\right)}, \tag{1}$$

where r_c is the critical distance for orbital overlap and β denotes the barrier steepness. Crucially, these parameters are determined by the liquid's specific electron affinity and work function. Therefore, any alteration in the liquid's molecular composition, such as the ratio of alcohol to water or the degradation of organic compounds, will fundamentally shift this transfer probability.

Electric Double Layer (EDL) Formation: The transferred electrons do not exist in isolation. Instead, they create a surface field that attracts counter-ions from the liquid, forming the EDL [28]. The structure of this layer dictates how the surface charge is screened. Mathematically, the electric field within the EDL is described by the Poisson-Boltzmann equation [19]:

$$\nabla \cdot \mathbf{E} = \nabla^2 \psi(x) = -\frac{\rho_e}{\varepsilon}, \tag{2}$$

where $\psi(x)$ is the potential distribution and ε is the permittivity of the liquid. The charge density ρ_e is directly determined by the ion valency z_i, the elementary charge e, and the concentration c_i: $\rho_e = \sum_i z_i e c_i$. Simultaneously, the dynamic movement of ions to form this layer is governed by the Nernst-Planck equation for ion flux: $\mathbf{J}_i = -D_i \nabla c_i + z_i \mu_i c_i \mathbf{E}$, where D_i and μ_i represent diffusivity and mobility. By solving these governing equations, we derive the critical characteristic scale of the EDL, *i.e.*, the *Debye Length* (λ_D):

$$\lambda_D = \sqrt{\frac{\varepsilon k_B \mathcal{T}}{\sum_i z_i^2 e^2 c_i}}, \tag{3}$$

where k_B is the Boltzmann constant and $\mathcal{T}$ is the temperature. Equation 3 establishes the *ionic fingerprint*. A higher ion concentration c_i reduces λ_D. Crucially, this thinner layer results in a higher interfacial capacitance $C \approx \varepsilon A/\lambda_D$ (where A is the contact area), making the electrical response highly sensitive to liquid concentration.

Saturation: The process culminates in a self-regulating feedback loop. The accumulated charge $Q(t)$ generates an interfacial potential difference $\phi = Q(t)/C$, which acts as an energy barrier opposing further electron transfer. Consequently, the electron transfer rate $\Gamma_e(t)$ evolves as:

$$\Gamma_e(t) = k_e \cdot T(r(t)) \cdot \varphi(r(t)) \cdot \exp\left(-\frac{e\phi}{k_B \mathcal{T}}\right). \tag{4}$$

Here, k_e is the kinetic transfer coefficient, and $\varphi(r(t))$ represents geometric factors such as effective collision frequency. $\exp(-e\phi/k_B\mathcal{T})$ represents the suppression effect of the established EDL potential. This equation reveals that the final accumulated charge $Q(t)$ is not random. It is the unique solution determined by the liquid's molecular nature ($T(r)$) and ionic concentration (via C and ϕ). This ensures that distinct liquids exhibit distinct charge transfer behaviors.

3.2 Feasibility Study

LSI for Liquid Verification: As illustrated in Fig. 3, the signal generation is governed by the coupling of contact electrification and electrostatic induction. ❶ Initially (Fig. 3(a)), when the liquid rests against the container wall, CE creates a layer of bound charges on the inner solid surface, which attracts counter-ions in the liquid to form the EDL. These induced charges remain static, maintaining an electrostatic equilibrium with the ground. ❷ Subsequently, when the bottle undergoes mechanical motion (Fig. 3(b)), such as rotation, the effective liquid-solid contact area changes. This physical disturbance disrupts the electrostatic balance. Since the total induced charge on the tag is proportional to the contact area covered by the EDL, the variation in contact area creates a potential difference between the tag and the ground. ❸ To re-establish equilibrium (Fig. 3(c)), electrons are driven through the external circuit, generating a transient current $I(t)$. As the liquid continues its motion or returns to a stable state, the charges redistribute, causing the current to flow continuously to track the motion.

Since the charge density is determined by the ionic strength (affecting the Debye length λ_D) and molecular affinity (affecting r_c), different liquids induce different magnitudes of charge for the same mechanical motion. For instance, a liquid with a higher ion concentration compresses λ_D. While this increases interfacial capacitance, the dense mobile ions create a stronger *screening effect* that confines the electric field within the EDL, thereby reducing the net potential perceived by the external tag. Consequently, by monitoring the current $I(t)$, which is the time derivative of the accumulated charge $Q(t)$, we directly infer the unique electrochemical fingerprint of the liquid.

Feasibility Experiments: We present a preliminary experiment to validate the capability of *AquaCode* in two critical dimensions of verification, *i.e.*, **sensitivity to quality deviations** (*e.g.*, dilution) and **discriminative power against substitution** (*e.g.*, counterfeiting).

First, to examine the sensitivity to concentration changes, we test Sodium Chloride (NaCl) solutions with varying concentrations as a proxy for dilution or spoilage. Fig. 4a plots the integrated signal magnitude against concentration. The results reveal a sharp and monotonic response where the signal intensity drops precipitously from 1239 to 129 as the ion concentration increases from 0.9%

to 30%. This trend aligns with the ionic screening theory since higher concentration strengthens the EDL screening and effectively suppresses the induction signal. Such a drastic signal shift confirms that even minor deviations from the standard concentration of a product create a detectable gap for verification.

Furthermore, a robust verification system must reject substitutions where the liquid is chemically altered but visually similar. Fig. 4b compares the time-domain waveforms of varying NaCl solutions against a glucose solution. The difference is fundamental. While high-concentration NaCl exhibits a flattened signal due to strong screening, the glucose solution is driven by molecular polarization rather than ionic dynamics. Consequently, it generates a distinct waveform with specific phase and shape characteristics. This observation confirms that LSI captures a rigid physicochemical fingerprint. Even if a counterfeiter substitutes a saline product with a sugar-based solution to mimic physical properties like density, the resulting signal fails to match the reference waveform and ensures effective rejection.

3.3 Entry Points of Design

While leveraging LSI for liquid quality check holds significant promise, the design is still challenging. These challenges dictate our specific design choices across the sensing interface, hardware readout, and algorithmic logic.

Excitation and Motion Artifact: The first challenge lies in establishing a reliable, active communication channel between the internal liquid and the external reader. This faces two physical barriers: 1) The LSI charges are generated on the *inner* wall, physically isolated by the container's glass or plastic shell. A naive solution might employ active sensors inside, but this is invasive and economically prohibitive for low-margin retail goods. 2) As noted in § 3.1, the interface naturally tends toward electrostatic equilibrium. A stationary bottle is electrically silent regardless of its contents. However, motion is a double-edged sword. In traditional sensing, stochastic human handling acts as a major source of motion, yet introducing motion artifacts that bury the liquid's signature. Since the signal depends on both motion and liquid properties, random motion makes reliable verification complicated. To address this, we must incorporate a specific tag design to bridge the dielectric barrier via capacitive coupling. Simultaneously, we must leverage the checkout platform to render the motion deterministic, decoupling the motion artifacts from the liquid's response.

Ultra-High Impedance Signal Acquisition: Even with an active coupling interface, acquiring the LSI signal presents a severe electrical challenge due to extreme impedance mismatch. The LSI source behaves essentially as a capacitor with an internal impedance exceeding 100 $G\Omega$. In contrast, conventional data acquisition interfaces (*i.e.*, standard Op-Amps) typically present input impedances in the $M\Omega$ range. As demonstrated in Fig. 5, this mismatch is catastrophic. Connecting the tag directly to an ADC results in a dead signal, as the low-impedance load instantly drains the induced charge. On the other hand, even with amplification, standard electronics fail due to input bias currents, which overwhelm the faint nano-ampere LSI currents, causing severe drift and saturation. So a generic readout circuit is fundamentally unsuitable [5, 10]. We must design a custom analog front-end featuring an electrometer-grade

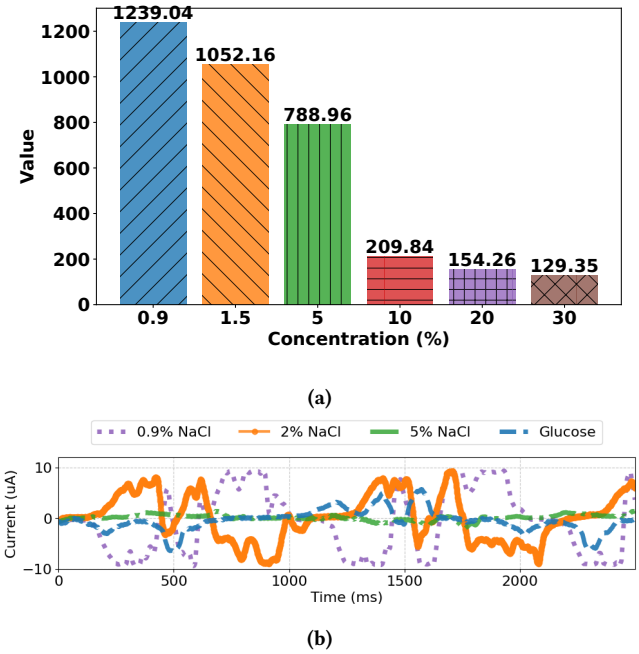

Figure 4: Feasibility Study

topology. This module must provide ultra-high input impedance and extremely low bias current to recover the high-fidelity waveform.

Scalable Physicochemical Interpretation: Finally, we need to transform raw signals into a verification decision. Counterfeiting is essentially an adversarial and open-set problem. While the genuine product is known, the potential variations of counterfeits (*e.g.*, dilution ratios, foreign additives, or chemical substitutions) are infinite and unpredictable. Supervised learning models, which require training on specific negative samples, inevitably fail when encountering a novel counterfeit type that was not present in the training set. To bridge this gap, we propose a physics-aware feature extraction mechanism. Instead of relying on opaque neural networks, we design an algorithm that fully exploits the LSI physics to inversely map the waveform back to interpretable physical parameters. We are supposed to achieve a robust, training-free verification model that establishes a golden standard based on causality rather than correlation.

4 *AQUACODE* DESIGN

The overall skeleton of *AquaCode* is depicted in Fig. 6. At a high level, we present a hardware-software co-design to effectively collect the LSI signals and conclude with a quantitative metrics for the liquid.

4.1 LSI Excitation

As discussed in 3.3, obtaining intrinsic liquid characteristics requires breaking the electrostatic equilibrium at the LSI. To induce charge transfer, we must introduce a mechanical disturbance that dynamically alters the charge distribution.

Physical Mechanism: When the liquid moves relative to the container wall, it disrupts the EDL structure. Microscopically, this mechanical energy perturbs the ionic arrangement at the interface. We

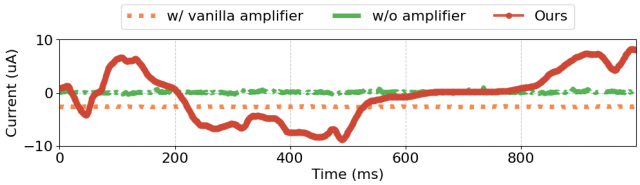

Figure 5: Comparisons of different amplifiers

model this disturbance as an oscillatory variation in the effective interaction distance, *i.e.*,

$$r(t) = r_0 + \Delta r \sin(\omega t), \tag{5}$$

where $r(t)$ is the distance between atoms at the LSI. This oscillation modulates the electron transfer rate, driving periodic changes in the accumulated charge $Q(t)$. Furthermore, the macroscopic fluid displacement shifts the diffuse layer relative to the solid surface, modifying the charge density distribution, *i.e.*,

$$\rho_e(z,t) = \rho_0 \exp(\frac{-z}{\lambda_D}) \cdot O(\sin(\omega t)) \tag{6}$$

where $O(\cdot)$ is the lateral distribution function of the rotating displacement. Consequently, the internal electric field changes dynamically, generating a measurable displacement current in the external circuit.

Motor-Driven Excitation: While various forms of mechanical displacement can theoretically disrupt the electrostatic equilibrium at the LSI, relying on human initiated movements introduces significant stochastic artifacts and non-uniform kinetic profiles that vary across individuals and sessions. Our key insight is, instead of employing a random motion artifact, we can make use of the controlled environment of the checkout platform. We incorporate a motor-driven module to provide standardized mechanical excitation [33]. Unlike random shaking, our system executes a precise inversion cycle: the container is rotated from an upright orientation (cap-up) to an inverted one (cap-down) and back. The inversion maximizes the change in the liquid-tag contact area A, thereby maximizing the generated signal amplitude and SNR. Moreover, by unifying the rotation speed and angle, the motion artifact becomes a constant, known variable that can be systematically decoupled from the liquid's response.

Deployment rationale of motor-based excitations: Here we justify our deployment rationales. First, the motor-based excitation mechanism is not rare in previous works [12, 33]. Importantly, many modern checkouts already possess the necessary mechanical motors and power systems (*e.g.*, conveyor belts). *AquaCode* can be integrated as a sensing module to reuse its motion as a controlled excitation source. Moreover, such an installation is a one-time effort with minimal long-term costs that benefits all stakeholders, including the manufacturers, retailers, and customers. Concretely, a commodity vibration motor costs <$20, negligible compared to retailers' IT budgets and losses from liquid fraud/spoilage. Furthermore, the rise of embodied robotics means that controlled mechanical interactions will likely become a native part of the checkout pipeline.

4.2 Hardware Design

4.2.1 Sensing Interface Design. The next step is to capture the microscopic charge transfer generated at the LSI. To harness this signal, we require a transducer capable of coupling with this dynamic field and translating the mechanical energy into a measurable electrical current. Since the LSI charges are generated on the inner wall, the container shell effectively acts as a dielectric layer. To capture the signal non-invasively, we implement a capacitive coupling **sensing tag** on the container's exterior.

As shown in Fig. 8a, we incorporate a simple metal tape (*e.g.*, copper or nickel foil) as the sensing electrode. Functionally, this tag serves as the external plate of a capacitor. As the internal electric field fluctuates due to the rotation-induced EDL perturbation, it induces a displacement current on this external metal tag through the container wall. The material is ubiquitous, flexible, and chemically stable, allowing it to conform to curved surfaces and blend into standard packaging lines. Most importantly, the cost is minimal, enabling scalability. Metal tape costs less than 1 cent per unit, and since it is mass-produced and already part of the packaging, scaling up for larger applications is cost-effective.

4.2.2 Analog Frontend. Due to the extremely high internal impedance of LSI, standard voltage amplifiers fail to measure the signals accurately due to impedance mismatch, as discussed in §3.3 and Fig. 5. While existing works [16, 42] share the underlying principle of contact electrification, their hardware objectives are fundamentally different, where they are designed to store or consume the charge for harvesting. Rather, AquaCode is to capture the LSI "signature" with maximum fidelity, prioritizing signal integrity over energy quality. To this end, we design a specialized analog frontend to capture the faint charge transfer at the LSI. This circuit fulfills two critical tasks: impedance matching and signal amplification.

We present our core design in Fig. 7. At the heart of the frontend is the Transimpedance Amplifier. It leverages a negative feedback loop to force the inverting input to match the potential of the non-inverting input. Since the non-inverting input is grounded, the inverting input becomes a "virtual ground." This allows the sensor to discharge its current freely and instantly without being impeded by the measurement circuit. The output voltage from the amplifier is governed by the feedback resistor R_f:

$$V_{o1} = -I_{\text{LSI}} \cdot R_f, \tag{7}$$

where I_{LSI} is the source current from the LSI, and R_f determines the transimpedance gain. We choose $R_f = 100\,\text{M}\Omega$, such that a minute current of 1 nA is amplified into a 0.1 V output. Simultaneously, a capacitor C_f is placed in the feedback loop for two purposes. First, given the high sensitivity of the LSI, the op-amp input is susceptible to parasitic capacitance, which can cause oscillation or ringing. C_f provides a high-frequency path to compensate for the phase margin and stabilize the amplifier. Second, it forms a first-order low-pass filter with R_f, with a cutoff frequency given by:

$$f_c = \frac{1}{2\pi \cdot R_f \cdot C_f}. \tag{8}$$

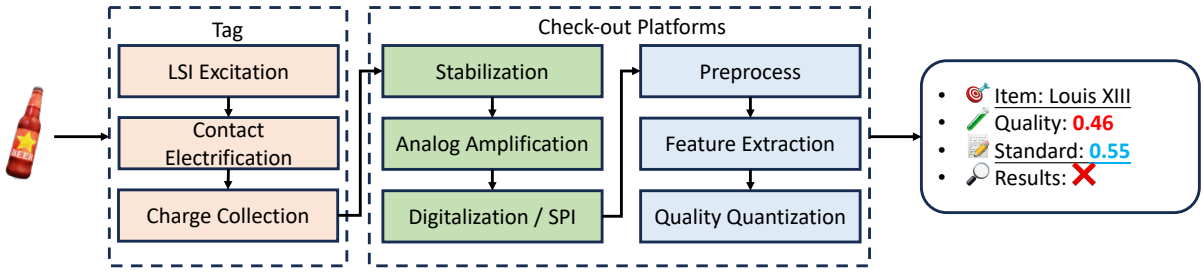

Figure 6: Overall Pipeline of *AquaCode*

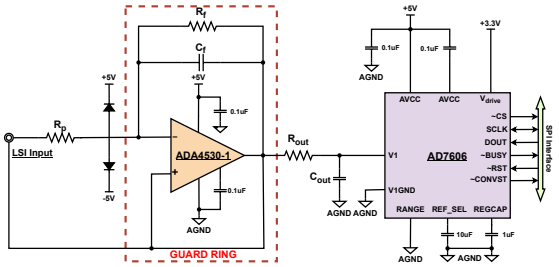

Figure 7: Analog Frontend Design

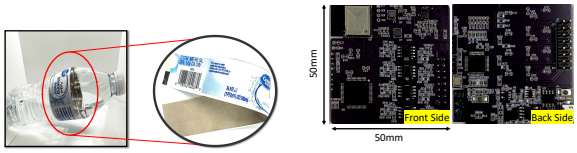

(a) Smart Tag **(b) Hardware Prototype**

Figure 8: Implementation of the Hardware

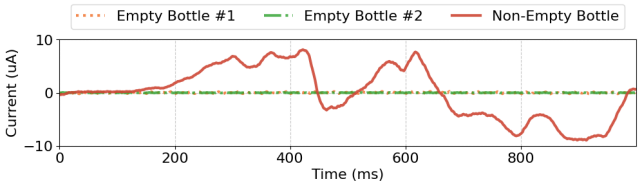

Figure 9: LSI Effect w/o and w/ Liquid.

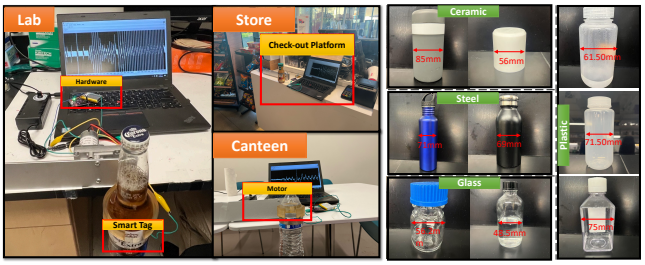

Figure 10: Experiment Setup. Left: Data collected at different places; Right: Data collected with containers of different sizes, shapes and materials.

This filters out high-frequency noise beyond the signal bandwidth. We select $C_f = 10\,\text{pF}$, resulting in a cutoff frequency of approximately 160 Hz. Additionally, to protect the op-amp from high-voltage static electricity generated by the LSI, we incorporate a protection resistor $R_p = 10\,\text{k}\Omega$ and low-leakage clamping diodes at the input. When the input voltage exceeds the safety threshold, the diodes conduct to discharge the excess energy.

After the amplification stage, the voltage signal passes through a passive RC filter composed of a resistor $R_{\text{out}} = 100\,\Omega$ and a capacitor $C_{\text{out}} = 1\,\text{nF}$. This stage serves as an anti-aliasing filter and absorbs the charge kickback from the subsequent sampling circuits. Finally, the conditioned analog signal is fed into a 16-bit bipolar ADC. Unlike unipolar ADCs that require DC biasing, the bipolar ADC supports a ±5 V input range, allowing direct coupling with the TIA output without additional level-shifting circuitry. The ADC samples the signal at a rate of 1 kHz and transmits the digitized data to the MCU via the SPI interface for further processing.

We implement two critical strategies to suppress leakage currents and power noise. First, we incorporate a guard ring structure around the sensitive inverting input node, the feedback resistor, and the feedback capacitor. The guard ring is a bare copper trace connected to the guard pin of the op-amp, driving the ring to the same potential as the input node. According to Ohm's law, maintaining a zero potential difference between the guard ring and the input terminal effectively nulls surface leakage currents, ensuring that all current flowing through R_f originates solely from the sensor.

Second, we employ a robust power decoupling network. For the op-amp, 0.1 μF ceramic capacitors are placed close to the ±5 V power pins to minimize trace inductance. For the ADC, a 10 μF capacitor is connected to the reference pin, serving as a charge reservoir to stabilize the internal voltage reference and minimize quantization noise.

Fidelity Validation: We conduct a control experiment as shown in Fig. 9. The objective is to verify that the recorded signals stem from genuine interface charge transfer rather than instrument noise or drift. We perform measurements on a bottle containing NaCl solution and compared the results against two empty control bottles. The results demonstrate that the measurements with the liquid present exhibit distinct, meaningful signal patterns corresponding to the LSI, whereas the empty bottles show only a flat baseline noise floor centered around zero. This confirms the high signal-to-noise ratio and reliability of our frontend design.

4.3 Quantitative Metrics

We visualize the measured $I(t)$ as illustrated in Fig. 11. As can be seen, despite diverse patterns across different liquids, $I(t)$ fundamentally differ for different liquid qualities. To this end, we focus on the measured $I(t)$ for feature extractions.

4.3.1 Feature Extractions. The features are embedded in the current. Since the trigger is changing the electron transfer direction,

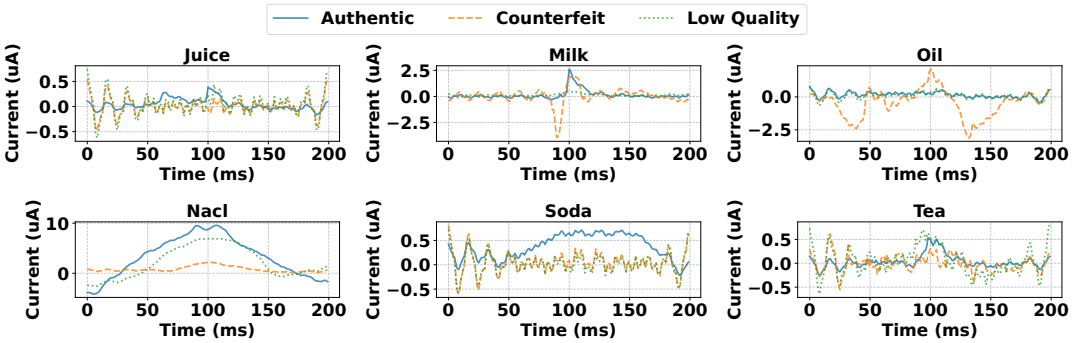

Figure 11: Visualization of Current for Liquids with Various Quality.

the current is oscillating quasi-periodically. Therefore, we choose the absolute integration of $I(t)$, *i.e.*, $\mathcal{M}_I \triangleq \int_{t_{w_s}}^{t_{w_e}} |I(t)|\, dt$. where t_{w_s} and t_{w_e} represent the start and end time of the clip window. Meanwhile, we can think from the energy's perspective, *i.e.*, how many energies are transferred at the LSI. Here the power source is the mechanical potential that water brings. Therefore, we can use the Root Mean Square (RMS), $\mathcal{M}_R \triangleq \sqrt{\frac{1}{t_{w_e}-t_{w_s}} \int_{t_{w_s}}^{t_{w_e}} I^2(t)dt}$. Additionally, we find that the peak-to-peak amplitude is helpful in identifying the liquid, as it reflects the atomic polarizations and quantifies the dynamic range of the signal. Therefore, we define $\mathcal{M}_p \triangleq I_{\max}(t) - I_{\min}(t)$, where $t \in [t_{w_s}, t_{w_e}]$.

4.3.2 Liquid Quality. To classify liquids based on the extracted features $\mathcal{M}_I$, $\mathcal{M}_R$, and $\mathcal{M}_p$, we employ a two-step methodology that leverages both individual and combined feature representations for robust identification. Initially, we aggregate the features in two distinct ways. First, we stack $\mathcal{M}_I$, $\mathcal{M}_R$, and $\mathcal{M}_p$ into the feature vector, preserving their individual contributions and allowing the classifier to assess their unique significance. Second, we compute a weighted sum, defined as $\mathcal{M}_c = w_I\mathcal{M}_I + w_R\mathcal{M}_R + w_p\mathcal{M}_p$, where w_I, w_R, and w_p are predefined hyperparameters. This composite representation integrates the features into a unified metric, enhancing classification robustness by capturing their collective effect. The integrated metric can be viewed as a quantitative quality assessment feature. Ideally, we can acquire the feature vector $\mathcal{M}$ for each data. Then we set a threshold ϵ_i for every single metric. If the distance between them is larger than ϵ_i, we deem it as a low-quality sample.

4.3.3 Preprocess. As the LSI inherently relies on rotation-triggered interactions, preprocessing is to ensure robustness against variability. The rotation can vary in amplitude, frequencies and angles, which contribute to the acquired $I(t)$. However, motor interference occurs at a predictable fundamental frequency. Because the LSI signal represents a broader electrochemical spectrum the motor frequency can be isolated using narrow-band notch filtering without losing critical quality information. To this end, a band-pass filter is applied to eliminate high-frequency noise from ambient vibrations and low-frequency drift caused by rotational speed fluctuations. This preserves the spectral features critical for classification while suppressing non-informative interference. Additionally, a sliding window approach segments the time-series data into overlapping intervals, enabling the system to capture stable, localized patterns even during rotational speed transitions. By isolating

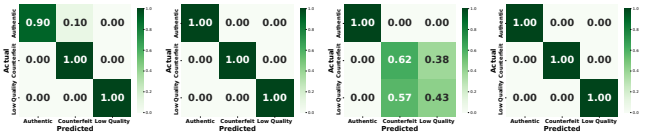

(a) Tea **(b) Juice** **(c) Soda** **(d) Milk**

Figure 12: Confusion Matrix of Common Drinks

rotation-invariant features and averaging transient disturbances, this preprocessing pipeline ensures consistent performance across diverse operational conditions.

5 IMPLEMENTATION

Hardware Prototype: We prototype the charge amplification module hardware into a dedicated PCB design using Altium Designer 18, as shown in Fig. 8b. We select the ADA4530-1 op-amp for its compact SOIC-8 package, high input impedance, and low noise characteristics, making it ideal for our design. The AD7606 ADC module is chosen for its precision in converting analog signals to digital signals. The IP5306 power management IC handles charging ion batteries and supplying power. The hardware module is compact, measuring only 5cm in width and height. We use the STM32 L431 microprocessor, based on the ARM Cortex-M4 core. It supports SPI for connecting to the AD7606 ADC and I2C for managing the IP5306 power management IC. For wireless communication, we add an ESP32 module. In our prototype, the bottle is placed on a motorized holder. A conductive connector on the holder touches the sensing tag attached to the bottle and collects the signal. This signal is sent through a short wire to the PCB for amplification and digitization, and the PCB then wirelessly transmits the data to the computer.

Software Implementation: We implement the upper program using LabView in the laptop, which is commonly used in the checkout systems. The LabView has a Virtual Instrument programmed to listen for incoming data from the ESP32. We use UDP to receive the data for processing. The data is visualized in real-time, providing instant feedback to users or the checkout system. Afterwards, we use Python to extract the features and evaluate the quality, where the sampling rate is 100Hz. The computations are done on a Thinkpad T460 with Intel® Core™ i5-6300U Processor.

Data Collection: To ensure a stable charge output from the LSI, we use a reduction gear motor with adjustable speed and a rocker actuator for continuous rotation. The rotation takes less than 2 seconds.

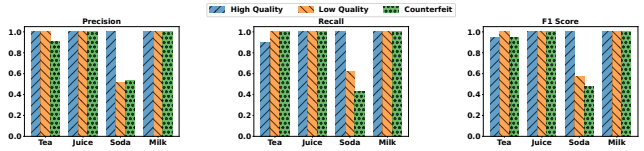

Figure 13: Performances of Common Drinks

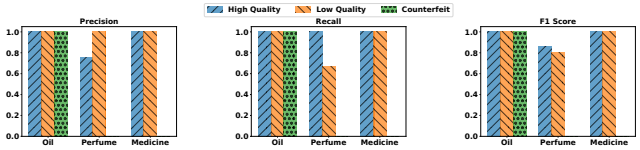

Figure 14: Performances of Other Liquids

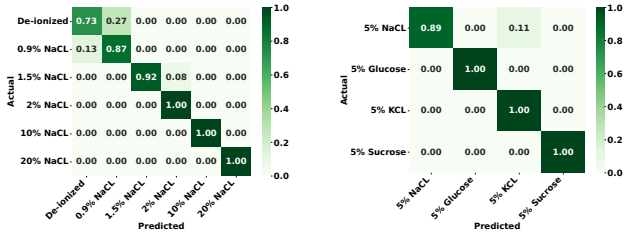

(a) Different Resolutions **(b) Same Density**

Figure 15: Varying Reagents

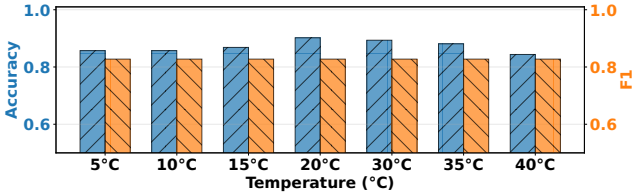

Figure 16: Varying Temperatures

We also use 3D printing to make a container holder with a spring mechanism to adapt to various volumes. Each rotation of the liquid constitutes one cycle. To comprehensively assess the robustness of the system, we collect and test common liquids as well as their low quality versions (diluted 10% by water) and fake liquids [11, 21, 33]. Low-quality samples are designed to mimic common adulteration methods such as dilution or ionic imbalance which are typical in counterfeit liquid products. We also investigate the system's resolution by precisely configuring different concentrations of sodium chloride solutions and examined the stability of feature extraction by varying the motor's rotation frequency. Additionally, we test the system's universality by using different types and shapes of containers, including glass, ceramic, and stainless steel containers, as depicted in Fig. 10.

6 EVALUATION

In this section, we elaborate on our experiments and evaluations. At a high level, we set up the standard metric for each liquid, and compared the testing liquid with the standard liquid using Euclidean distance. Notably, we target 1-to-1 SKU verification rather than general liquid classification. Each product line carries a unique "LSI signature", with a manufacturer-defined reference metric and tolerance threshold stored in the product's identity tag. To validate our liquid quality metric, we map them into "high quality", "low quanlity" and "counterfeit, and compare the accuracy of the mapping. We additionally introduce low-quality samples to quantify the system's sensitivity margin, *i.e.*, how the verification boundary can be tightened or relaxed to detect intermediate degradations. This demonstrates that *AquaCode* is a manufacturer-configurable verification tool rather than a generic classifier.

These metrics are widely used in to assess the model's accuracy, robustness, and generalization capability. Besides these evaluations, we conduct a user study shown in §6.3.

6.1 Overall Performance

6.1.1 Common Drinks. We first evaluate our performances across the common drinks, including tea, juice, soda drink, and milk. As can be seen from Fig. 12, we illustrate the confusion matrix of those common drinks. As can be seen from the confusion matrix, the system performs well in distinguishing the common drinks. For tea, we achieve a precision of 1.00, a recall of 0.90, and an F1 score of 0.95 in identifying high-quality tea. We also successfully identified all low-quality tea samples. For fake tea, we achieve a precision of 0.91, a recall of 1.00, and an F1 score of 0.95. For juice, we correctly identify all high-quality, low-quality, and fake juice samples. While distinguishing between low-quality and fake soda is challenging, we achieve a precision of 1.00 for authentic soda, ensuring consumers can select authentic soda and avoid low-quality or fake ones. For milk, we achieve a precision of 1.0 for identifying high-quality, low-quality, and fake milk samples. The precision, recall, and F1 results are summarized in Fig. 13. Overall, we achieve an average recall of 0.975±0.043 for identifying high-quality drinks and an average recall of 0.905±0.165 for detecting low-quality drinks.

6.1.2 Other Liquids. We then evaluate other common liquids, including oils, perfumes and medicines.

Oils: We define low-quality oils as adding impurities to the Olive Oil while high-quality oils as identifying Peanut Oil. As can be seen from Fig. 14, we distinguish them with the recall and F1 score of 1.00. This means that we can accurately identify the authentic Olive Oil and prevent the consumers from purchasing the low-quality Olive Oil. Furthermore, we achieve a precision of 1.00 in identifying the fake Olive Oil.

Perfume: We then test the perfumes. We add deionized water to the perfume to create low-quality samples. Notably, we achieve F1 score of 0.86 in identifying the authentic perfume while that for the low-quality perfume is 0.80. All the predicted low-quality perfumes are indeed with low quality, demonstrating the high precision of our metrics.

Medicines: The quality of liquid medicines is also vital. We prepare the low-quality drugs by adding another type of syrup to the medicinal liquid. From the Fig. 14, it can be seen that our quality indicators can very accurately identify low-quality and high-quality drugs. We achieve a precision of 1 and a recall of 1. This demonstrates the role of our indicators in facilitating drug quality detection.

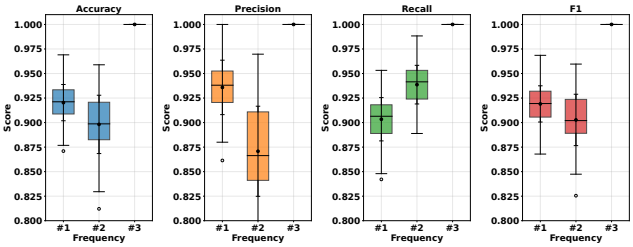

Figure 17: Varying Rotating Frequency

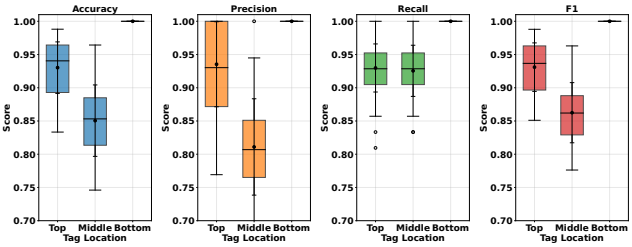

Figure 18: Varying Tag Locations

6.2 Benchmark Study

6.2.1 Different Resolutions. We first study the performance of distinguishing different concentrations of NaCl. The proposed approach demonstrates strong performance in identifying various NaCl concentrations, achieving an overall accuracy, precision, recall, and F1 score of 0.92 each (Fig. 15a). At higher concentrations, the LSI achieves 100% precision, recall, and F1 scores. At concentrations of 1.5% and 2%, the quality metric also shows excellent performance, with F1 scores of 0.96, underscoring the effectiveness in capturing liquid features. However, there are opportunities to refine its handling of close-concentration classes. For instance, the de-ionized water (DI) class exhibits a recall of 0.73, suggesting the potential to enhance sensitivity. Similarly, the 0.9% NaCl class shows a precision of 0.76, indicating minor ambiguity in boundary cases that could be addressed through targeted adjustments. These observations highlight pathways to further elevate the system's reliability, particularly for subtle distinctions at lower concentrations.

6.2.2 Different Reagents. We then study the quality measurement for different solutions with the same density, as shown in Fig. 15b. Overall, it achieves an accuracy of 0.97, with precision, recall, and F1 score all at 0.98, 0.97, and 0.97, respectively. For the 5% NaCl solution, the quality metrics reveal a precision of 1.00 and a recall of 0.89, resulting in an F1 score of 0.94. Additionally, the confusion matrix shows that 11% of the 5% NaCl samples were misclassified as 5% KCL. Moreover, the proposed approach achieves perfect performance for 5% glucose and 5% sucrose solutions, with both precision, recall, and F1 scores at 1.00. This indicates that the LSI interface successfully captures the unique characteristics of these solutions, enabling flawless differentiation. Similarly, the 5% KCL solution also exhibits excellent performance, with a precision of 0.90 and a recall of 1.00, leading to an F1 score of 0.95. These results justify the robustness and consistency of our quality metrics across different liquids.

6.2.3 Varying Temperatures. We study the influence of temperature, as shown in Fig 16. We measure the metrics of temperature from 5°C to 40°C, where the threshold is derived from room temperature (25°C). As we can see, the accuracy and F1 score remain stable across the temperature range, with both metrics staying around 0.9. The performance peaks near the baseline temperature and decreases symmetrically. Note that it is reasonable to witness some accuracy drops, as the temperature is one of the impact factors of the LSI. We will discuss it in §8.

6.2.4 Varying Rotating Frequencies. The proposed processing method effectively mitigates rotational frequency interference, enabling robust LSI interface performance across all tested configurations, as shown in Fig. 17. At a reduced rotational speed (Configuration #1), the system achieved 92% accuracy with precision of 0.94 and recall of 0.90. Configuration #2 maintained 89% accuracy with modest misclassifications. Configuration #3 achieved 100% accuracy, precision, recall, and F1 score, highlighting the method's ability to optimize sensor-solution interactions under ideal rotational conditions. These results validate the preprocessing pipeline's effectiveness in filtering frequency-related noise, ensuring reliable performance across diverse operational settings.

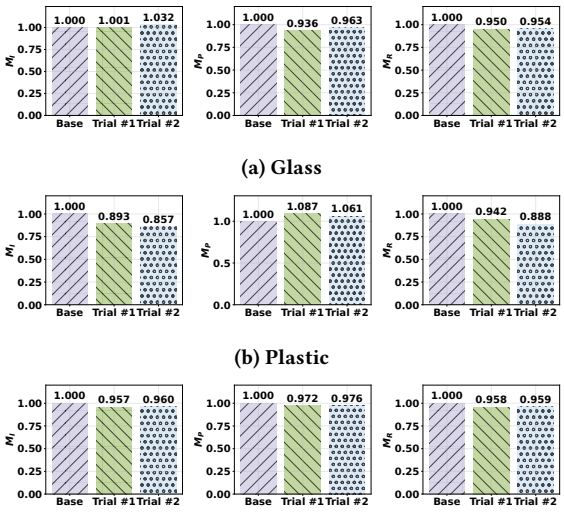

(a) Glass

(b) Plastic

(c) Steel

Figure 19: Stability of Different Materials

6.2.5 Varying Tag Locations. The impact of tape placement on the LSI interface's performance is evaluated across three positions: top, middle and bottom. We depict the results in Fig. 18, which confirms that tape placement has minimal influence on classification reliability. For the top placement, the system achieved 93% accuracy with balanced precision, recall, and F1 scores of 0.93 each. This indicates that positional adjustments do not significantly disrupt signal stability or feature discriminability. The middle placement showed a slight reduction in accuracy to 85% and precision to 0.81. The bottom placement delivered 100% accuracy and perfect metric scores, reinforcing the system's robustness. Tag placement at the bottom of the container yields superior results because gravity ensures maximum contact pressure and contact area between the liquid and the sensor interface. These minor fluctuations underscore the effectiveness of the charge collection and amplification

module in stabilizing signals and suppressing positional noise. The LSI consistently maintains performance across diverse tape locations, validating its adaptability to deployment-specific variations. Notably, in practical scenarios, the manufacturer will specify the exact location of the identity tag during the manufacturing process. This allows them to strategically select the placement that yields the highest SNR and the most distinct electrochemical signature for a given SKU. By standardizing this location at the point of production, the system ensures that the measured response is always compared against a reference generated under identical physical configurations.

6.2.6 Non-cylindrical Bottles. To validate that LSI works for every surface, we evaluate our system on non-cylindrical bottle shape, *i.e.*, paper-based packaging. We achieve accuracy and F1 score of 0.909 and 0.872, respectively, demonstrating that LSI generalizes well to surface geometry.

6.2.7 Varying Materials. We study whether our metrics work well on different materials. We select three commonly used materials for off-the-shelf liquid containers: glass, steel, and plastic. Using data from the first test as our baseline, we compare the metrics recorded at various times using the same container material. The results are depicted in Fig. 19. We observe that for glass containers, metric variations are minimal, with the largest variations of $\mathcal{M}_P$, which changes 6.4%. Similar trends are observed in plastic and steel containers. Notably, the largest variation for plastic containers is an 11.2% change in $\mathcal{M}_R$ changes while steel containers exhibit a relative 4.3% decrease in $\mathcal{M}_I$. We achieve 100% accuracy for identifying the liquid in all three containers. These results demonstrate that our LSI design generalizes well across different materials, enabling liquid quality checks across various containers.

6.2.8 Stability. We investigate the stability of our metrics by analyzing experiments conducted on separate days. As shown in Fig. 19, our metrics remain relatively consistent across trials and materials. Additionally, we present a one-week stability study shown in Figure 20. The accuracy remain stable during this period, indicating that our proposed quantitative metrics are stable over time, making them suitable for adoption as industry standards by manufacturers and verification at checkout locations.

6.2.9 Overhead of AquaCode. To evaluate performance, we measure the overhead associated with *AquaCode*, including data acquisition from hardware, current signal processing, and final result comparison. Our results show that the total processing time per liquid is only 5.3 ms, with a memory buffer usage of just 0.45 MB. These findings demonstrate that our system is sufficiently lightweight to operate seamlessly on any transactional platform, ensuring it does not interfere with user experience.

6.3 User Study

To assess the effectiveness and user acceptance of our proposed system designed to enhance the retail shopping experience, we conduct a user study with 11 participants in a real retail environment. Following their interaction, participants are asked to complete a survey that collects data on their demographics, shopping habits, and perceptions of the system, as shown in Table 1.

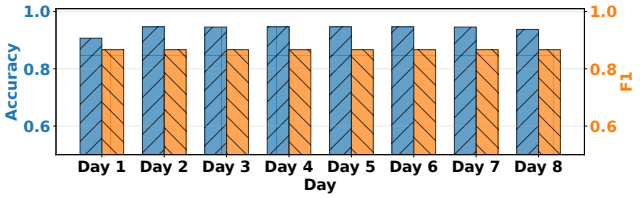

Figure 20: A One-week Stability Study

The participant group is diverse, ranging in age from 24 to 37 years old, with a nearly balanced gender distribution (6 males and 5 females). Shopping habits varied slightly: most participants (9 out of 11) report visiting retail shops 1-3 times per week, while one participant visits less than once a week, and another visits 4-7 times a week. This demographic spread provided a broad perspective on how the system might be received by typical retail consumers.

Survey results reveal that the system is generally safe and comfortable to use. 10 out of 11 participants report no electric shock sensations during the experiments, assigning a score of 1 (indicating "no" on a presumed 1-5 scale, where 1 is negative and 5 is positive). One participant provides a neutral score of 3, suggesting that while the system is safe for most, additional investigation might be warranted to ensure comfort for all users. When asked whether adding liquid detection at checkout would enhance their shopping experience, participants respond positively. 8 out of 11 strongly agree, assigning the highest score of 5, and one participant somewhat agrees with a score of 4. Two participants remain neutral with a score of 3, which underscores the perceived value of liquid detection as a beneficial feature in retail settings.

The system's impact on participants' normal shopping processes is minimal. 7 participants report no effect (score of 1), and two indicated a slight effect (score of 2). One participant gives a neutral score of 3, hinting that minor adjustments might improve the system's integration into existing shopping routines. Overall, these responses suggest that the system can be incorporated seamlessly into retail environments without significant disruption.

Finally, participants rate the new feature highly. 8 out of 11 give it the top score of 5, reflecting strong approval, while three assigned a neutral score of 3. This positive reception indicates that the feature is well-regarded, though the neutral responses suggest opportunities for refinement to fully meet all users' expectations.

In conclusion, the user study demonstrates that our system is well-received by the users, which offers a safe, non-disruptive, and valuable enhancement to the retail shopping experience. The overwhelmingly positive feedback on liquid detection and the high feature ratings highlight its appeal, while the few neutral responses provide insights for further optimization. These findings support the system's potential for practical implementation and suggest directions for future improvements to maximize user satisfaction.

7 RELATED WORK

Liquid Sensing: Liquid analysis has been explored through vision, acoustics, RF signals, and optical interrogation for applications in food safety, healthcare, and industrial monitoring [3, 4, 27, 44, 48]. Vision-based techniques use color and transparency features or container imaging [13, 33, 45], but typically require controlled lighting or container opening. Acoustic approaches analyze resonances or

Table 1: Questions of the User Study Survey

Question	Type
Your age	Numerical
Gender	Categorical (nominal)
How often do you go to retail shops?	Ordinal (frequency)
Did you experience any electric shock sensations during the experiments?	Ordinal (1-5)
Do you agree adding liquid detection at checkout would enhance your shopping experience?	Ordinal (1-5)
Do you feel that our system has affected your normal shopping process?	Ordinal (1-5)
As a consumer, how would you rate this new feature?	Ordinal (1-5)

impulse responses from tapping or external excitation [12, 21, 34, 43], while wireless-based systems use Wi-Fi [9, 29, 30], mmWave [22, 25, 38, 40] or RFID [11, 37, 41] to infer liquid properties. These systems show that non-invasive liquid interrogation is feasible, but they generally adopt a classification-centric framework and rely on channel-dependent features [11, 41] that vary across environments and hardware platforms. *AquaCode* differs fundamentally by performing verification using a manufacturer-defined golden reference and by leveraging an intrinsic, environment-invariant LSI signature rather than propagation-based measurements.

Liquid-Solid Interface: Electrification at material interfaces has been extensively studied, including solid-solid [6], solid-gas [35] and liquid-solid interface [16]. Most prior work investigates LSI for energy harvesting, particularly in marine environments or self-powered sensors [15, 20, 24, 42, 47], where the design goal is to maximize charge output from waves, droplets, or mechanical agitation. In contrast, *AquaCode* repurposes the LSI from an energy-harvesting mechanism to a sensing modality. Instead of optimizing power generation, we analyze how charge-transfer dynamics encode fine-grained physicochemical properties of liquids, and we design specialized hardware to non-invasively read these signals under standardized excitation. This positions *AquaCode* as a sensing-oriented reinterpretation of LSI technology, distinct from existing energy-focused literature. Additionally, we incorporate specialized hardware to enable non-invasive examination of LSI, even in scenarios with low SNR.

8 DISCUSSION AND FUTURE WORK

Deployment: The lack of quality checks at checkout leads to significant economic losses [1, 14]. We envision that all stakeholders have strong incentives to adopt our system. For manufacturers, integrating *AquaCode* can minimize contamination risks during liquid transportation. Retail shops can reduce liability risks. Consumers benefit from assurance regarding product quality. To achieve this vision, manufacturers could adhere the smart tag to their existing paper tape. Given the low cost of metal tape, this addition is economically viable compared to potential settlement fees from quality issues. For retail shops, the integration involves adding the hardware module to checkout platforms. This is a one-time effort with minimal long-term costs.

Mechanical Trigger: In this work, we leverage the rotation of the bottle to trigger the LSI. Such trigger can also be observed from previous works [12, 33]. Meanwhile, our LSI principle does not strictly require such a trigger. In fact, as long as we can disturb the equilibrium state of the charges at the surface, we are able to assess the transfer and, furthermore, evaluate the liquid quality. In future work, we aim to explore more effortless ways to assess liquid quality, such as by leveraging natural motions like the rolling of the bottle or capturing the vibrations caused when it is set down.

Threshold Selection: In this paper, our current thresholds are empirically tuned. That explains why our overall accuracy stays around 0.9. In fact, we anticipate that the manufacturers will take up the roles of setting up the threshold based on different liquid properties and container imperfections, as discussed in §2. Moreover, we envision our system a robust first layer of defense in retail environments, complementary with other existing methods to further improve the accuracy.

Temperature-Aware Check: Temperature is an important factor for the charge transfer behavior, as in Eq. (3). Fortunately, obtaining temperature data is relatively straightforward via refrigerator presets or affordable sensors (<$5). Practical calibration can utilize a simple infrared sensor to detect the bottle surface temperature and apply a linear correction factor to the measured signal.

Reliance on Conductivity: Although LSI amplitude correlates with conductivity, yielding weaker signals for dielectrics (*e.g.*, oils), our verification-based approach ensures effective detection. As shown in Fig. 11, any adulteration involving materials with distinct electrical properties triggers a detectable signal shift. Moreover, LSI captures the electrochemical shifts such as pH changes and protein denaturation that occur during real spoilage processes. Future work will explore additional feature dimensions to further enhance robustness for non-conductive liquids.

Impact of Container Material: *AquaCode* is inherently effective for dielectric containers (*e.g.*, glass, plastic) via capacitive coupling. While conductive metal cans could introduce electrostatic shielding, the internal LSI signal remains intact. Moreover, by leveraging our verification framework, the system is aware of the container type via the SKU. The system can then circumvent shielding through targeted adaptations, such as placing tags on plastic caps or utilizing the metal body itself as the sensing electrode.

9 CONCLUSION

This paper presents *AquaCode* that reframes liquid authentication from fragile channel-based classification to deterministic, physics-driven verification at retail checkout platforms. By leveraging intrinsic charge-transfer dynamics at the LSI and embedding a manufacturer-defined golden standard in a passive tag, *AquaCode* achieves a stable, environment-invariant liquid quality check that generalizes across products. Extensive experiments show an average recall of 0.975 for classifying authentic liquids and 0.905 for identifying low-quality drinks. Beyond this deployment, *AquaCode* opens a path toward infrastructure-supported quality assurance spanning food, pharmaceuticals, and logistics.

ACKNOWLEDGMENT

We sincerely thank the reviewers for their careful reading and valuable feedback. Sijie Ji is the corresponding author, and this work was supported by the Schmidt Science Fellowship.

REFERENCES

[1] AboutLawsuits.com. 2025. Similac Recall Over Liquid Formula Spoilage. https://www.aboutlawsuits.com/similac-recall-liquid-formula-spoilage/. Accessed: 2025.

[2] Sila Bozdag. 2023. Market analysis of smart checkout systems and iot payments. (2023).

[3] Justin Chan, Kelly Michaelsen, Joanne K Estergreen, Daniel E Sabath, and Shyamnath Gollakota. 2022. Micro-mechanical blood clot testing using smartphones. Nature communications 13, 1 (2022), 831.

[4] Justin Chan, Ananditha Raghunath, Kelly E Michaelsen, and Shyamnath Gollakota. 2022. Testing a drop of liquid using smartphone LiDAR. Proceedings of the ACM on Interactive, Mobile, Wearable and Ubiquitous Technologies 6, 1 (2022), 1–27.

[5] Tao Chen, Yongjie Yang, Chonghao Qiu, Xiaoran Fan, Xiuzhen Guo, and Longfei Shangguan. 2024. Enabling hands-free voice assistant activation on earphones. In Proceedings of the 22nd Annual International Conference on Mobile Systems, Applications and Services. 155–168.

[6] Yanghui Chen, Xiong Pu, Mengmeng Liu, Shuangyang Kuang, Panpan Zhang, Qilin Hua, Zifeng Cong, Wenbin Guo, Weiguo Hu, and Zhong Lin Wang. 2019. Shape-adaptive, self-healable triboelectric nanogenerator with enhanced performances by soft solid–solid contact electrification. ACS nano 13, 8 (2019), 8936–8945.

[7] Ashutosh Dhekne, Mahanth Gowda, Yixuan Zhao, Haitham Hassanieh, and Romit Roy Choudhury. 2018. Liquid: A wireless liquid identifier. In Proceedings of the 16th annual international conference on mobile systems, applications, and services. 442–454.

[8] João Diogo Falcão, Carlos Ruiz, Adeola Bannis, Hae Young Noh, and Pei Zhang. 2021. Isacs: In-store autonomous checkout system for retail. Proceedings of the ACM on Interactive, Mobile, Wearable and Ubiquitous Technologies 5, 3 (2021), 1–26.

[9] Chao Feng, Jie Xiong, Liqiong Chang, Ju Wang, Xiaojiang Chen, Dingyi Fang, and Zhanyong Tang. 2019. WiMi: Target material identification with commodity Wi-Fi devices. In 2019 IEEE 39th international conference on distributed computing systems (ICDCS). IEEE, 700–710.

[10] Xiuzhen Guo, Long Tan, Tao Chen, Chaojie Gu, Yuanchao Shu, Shibo He, Yuan He, Jiming Chen, and Longfei Shangguan. 2024. Exploring biomagnetism for inclusive vital sign monitoring: Modeling and implementation. In Proceedings of the 30th Annual International Conference on Mobile Computing and Networking. 93–107.

[11] Unsoo Ha, Junshan Leng, Alaa Khaddaj, and Fadel Adib. 2020. Food and liquid sensing in practical environments using {RFIDs}. In 17th USENIX symposium on networked systems design and implementation (NSDI 20). 1083–1100.

[12] Yongzhi Huang, Kaixin Chen, Yandao Huang, Lu Wang, and Kaishun Wu. 2021. A portable and convenient system for unknown liquid identification with smartphone vibration. IEEE Transactions on Mobile Computing 22, 4 (2021), 1894–1911.

[13] Yongzhi Huang, Kaixin Chen, Lu Wang, Yinying Dong, Qianyi Huang, and Kaishun Wu. 2021. Lili: liquor quality monitoring based on light signals. In Proceedings of the 27th Annual International Conference on Mobile Computing and Networking. 256–268.

[14] Investopedia. 2025. The 5 Largest U.S. Product Liability Cases. https://www.investopedia.com/the-5-largest-u-s-product-liability-cases-4773418. Accessed: 2025.

[15] Dongdong Jiang, Guoxu Liu, Wenjian Li, Tiaozhao Bu, Yipu Wang, Zhi Zhang, Yaokun Pang, Shaohang Xu, Hang Yang, and Chi Zhang. 2019. A leaf-shaped triboelectric nanogenerator for multiple ambient mechanical energy harvesting. IEEE Transactions on Power Electronics 35, 1 (2019), 25–32.

[16] Feng Jiang, Liuxiang Zhan, Jin Pyo Lee, and Pooi See Lee. 2024. Triboelectric nanogenerators based on fluid medium: from fundamental mechanisms toward multifunctional applications. Advanced Materials 36, 6 (2024), 2308197.

[17] Yuechun Jiao, Jinlian Hu, Zitong Lan, Fusang Zhang, Jie Xiong, Jingxu Bai, Zhaoxin Chang, Yuqi Su, Beihong Jin, Daqing Zhang, et al. 2024. Exploring quantum sensing for fine-grained liquid recognition. arXiv preprint arXiv:2407.19656 (2024).

[18] SADIA Khanom, KAMAL KANTA Das, SOURAV Banik, and RASHED Noor. 2013. Microbiological analysis of liquid oral drugs available in Bangladesh. Int J Pharm Pharma Sci 5, 4 (2013), 479–482.

[19] Gene Lamm. 2003. The poisson–boltzmann equation. Reviews in computational chemistry 19 (2003), 147–365.

[20] Wenjian Li, Liqiang Lu, Ajay Giri Prakash Kottapalli, and Yutao Pei. 2022. Bioinspired sweat-resistant wearable triboelectric nanogenerator for movement monitoring during exercise. Nano Energy 95 (2022), 107018.

[21] Zhaohui Li, Wei Luo, Yongmin Zhang, Jianxi Chen, Yuanchao Shu, and Yaoxue Zhang. 2024. ASLiquid: Non-Intrusive Liquid Counterfeit Identification with Your Earphones. In Proceedings of the 22nd ACM Conference on Embedded Networked Sensor Systems. 41–53.

[22] Yumeng Liang, Anfu Zhou, Huanhuan Zhang, Xinzhe Wen, and Huadong Ma. 2021. FG-LiquID: A contact-less fine-grained liquid identifier by pushing the limits of millimeter-wave sensing. Proceedings of the ACM on Interactive, Mobile, Wearable and Ubiquitous Technologies 5, 3 (2021), 1–27.

[23] Shiquan Lin, Xiangyu Chen, and Zhong Lin Wang. 2021. Contact electrification at the liquid–solid interface. Chemical Reviews 122, 5 (2021), 5209–5232.

[24] Wenbo Liu, Liang Xu, Tianzhao Bu, Hang Yang, Guoxu Liu, Wenjian Li, Yaokun Pang, Chuxiong Hu, Chi Zhang, and Tinghai Cheng. 2019. Torus structured triboelectric nanogenerator array for water wave energy harvesting. Nano Energy 58 (2019), 499–507.

[25] Zijuan Liu, Xiulong Liu, Xinyu Tong, Xin Xie, Jiancheng Chen, Ming Yang, and Keqiu Li. 2025. MLiquID: Towards Mobile Liquid Sensing with COTS RFIDs. IEEE Transactions on Mobile Computing (2025).

[26] Veronica Mugoyela and Kennedy D Mwambete. 2010. Microbial contamination of nonsterile pharmaceuticals in public hospital settings. Therapeutics and clinical risk management (2010), 443–448.

[27] Tauhidur Rahman, Alexander T Adams, Perry Schein, Aadhar Jain, David Erickson, and Tanzeem Choudhury. 2016. Nutrilyzer: A mobile system for characterizing liquid food with photoacoustic effect. In Proceedings of the 14th ACM Conference on Embedded Network Sensor Systems CD-ROM. 123–136.

[28] Wolfgang Schmickler. 1996. Electronic effects in the electric double layer. Chemical reviews 96, 8 (1996), 3177–3200.

[29] Fei Shang, Panlong Yang, Dawei Yan, Sijia Zhang, and Xiang-Yang Li. 2024. LiqImager: Fine-grained Liquid Identification and Container Imaging System with COTS WiFi Devices. Proceedings of the ACM on Interactive, Mobile, Wearable and Ubiquitous Technologies 8, 1 (2024), 1–29.

[30] Fei Shang, Panlong Yang, Yubo Yan, and Xiang-Yang Li. 2022. LiqRay: Non-invasive and fine-grained liquid recognition system. In Proceedings of the 28th annual international conference on mobile computing and networking. 296–309.

[31] Fei Shang, Panlong Yang, Yubo Yan, and Xiang-Yang Li. 2023. Contactless and Fine-Grained Liquid Identification Utilizing Sub-6 GHz Signals. IEEE Transactions on Mobile Computing 23, 5 (2023), 4992–5008.

[32] SoftProdigy.com. 2023. Why Quality Assurance Services Build Customer Trust. https://softprodigy.com/why-quality-assurance-services-build-customer-trust/. Accessed: 2025.

[33] Bangjie Sun, Sean Rui Xiang Tan, Zhiwei Ren, Mun Choon Chan, and Jun Han. 2022. Detecting counterfeit liquid food products in a sealed bottle using a smartphone camera. In Proceedings of the 20th Annual International Conference on Mobile Systems, Applications and Services. 42–55.

[34] Xue Sun, Wenwen Deng, Xudong Wei, Dingyi Fang, Baochun Li, and Xiaojiang Chen. 2023. Akte-liquid: Acoustic-based liquid identification with smartphones. ACM Transactions on Sensor Networks 19, 1 (2023), 1–24.

[35] József Tóth. 1995. Uniform interpretation of gas/solid adsorption. Advances in colloid and interface science 55 (1995), 1–239.

[36] Donald Robert Uhlmann, B Chalmers, and KA Jackson. 1964. Interaction between particles and a solid-liquid interface. Journal of Applied Physics 35, 10 (1964), 2986–2993.

[37] Ju Wang, Jie Xiong, Xiaojiang Chen, Hongbo Jiang, Rajesh Krishna Balan, and Dingyi Fang. 2017. TagScan: Simultaneous target imaging and material identification with commodity RFID devices. In Proceedings of the 23rd Annual International Conference on Mobile Computing and Networking. 288–300.

[38] Zhu Wang, Yifan Guo, Zhihui Ren, Wenchao Song, Zhuo Sun, Chao Chen, Bin Guo, and Zhiwen Yu. 2024. Liqdetector: enabling container-independent liquid detection with mmwave signals based on a dual-reflection model. Proceedings of the ACM on Interactive, Mobile, Wearable and Ubiquitous Technologies 7, 4 (2024), 1–24.

[39] Zhong Lin Wang and Aurelia Chi Wang. 2019. On the origin of contact-electrification. Materials Today 30 (2019), 34–51.

[40] Chenshu Wu, Feng Zhang, Beibei Wang, and KJ Ray Liu. 2020. mSense: Towards mobile material sensing with a single millimeter-wave radio. Proceedings of the ACM on Interactive, Mobile, Wearable and Ubiquitous Technologies 4, 3 (2020), 1–20.

[41] Binbin Xie, Jie Xiong, Xiaojiang Chen, Eugene Chai, Liyao Li, Zhanyong Tang, and Dingyi Fang. 2019. Tagtag: Material sensing with commodity RFID. In Proceedings of the 17th conference on embedded networked sensor systems. 338–350.

[42] Yanqin Yang, Xinge Guo, Minglu Zhu, Zhongda Sun, Zixuan Zhang, Tianyiyi He, and Chengkuo Lee. 2023. Triboelectric nanogenerator enabled wearable sensors and electronics for sustainable internet of things integrated green earth. Advanced Energy Materials 13, 1 (2023), 2203040.

[43] Yanni Yang, Yanwen Wang, Jiannong Cao, and Jinlin Chen. 2022. HearLiquid: Nonintrusive liquid fraud detection using commodity acoustic devices. IEEE internet of things journal 9, 15 (2022), 13582–13597.

[44] Hui-Shyong Yeo, Gergely Flamich, Patrick Schrempf, David Harris-Birtill, and Aaron Quigley. 2016. Radarcat: Radar categorization for input & interaction. In Proceedings of the 29th Annual Symposium on User Interface Software and Technology. 833–841.

[45] Shichao Yue and Dina Katabi. 2019. Liquid testing with your smartphone. In Proceedings of the 17th annual international conference on mobile systems, applications, and services. 275–286.
[46] Jonghyuk Yun, Kyoosik Lee, Kichang Lee, Bangjie Sun, Jaeho Jeon, Jeonggil Ko, Inseok Hwang, and Jun Han. 2024. PowDew: Detecting Counterfeit Powdered Food Products using a Commodity Smartphone. In Proceedings of the 22nd Annual International Conference on Mobile Systems, Applications and Services. 210–222.
[47] Chuguo Zhang, Baofeng Zhang, Wei Yuan, Ou Yang, Yuebo Liu, Lixia He, Zhihao Zhao, Linglin Zhou, Jie Wang, and Zhong Lin Wang. 2022. Seawater-based triboelectric nanogenerators for marine anticorrosion. ACS Applied Materials & Interfaces 14, 6 (2022), 8605–8612.
[48] Siqi Zhang, Mayank Goel, and Justin Chan. 2025. DropleX: Liquid sensing on tablet touchscreens. arXiv preprint arXiv:2511.02694 (2025).